ACADEMIA ROMÂNĂ
Revue Roumaine de Chimie
https://www.icf.ro/rrch/

Rev. Roum. Chim.,
2022, *67*(1-2), 101–109
DOI: 10.33224/rrch.2022.67.1-2.09

Dedicated to the memory of
Dr. Emilian GEORGESCU (1946-2020)

SELECTED POTENTIAL ANTI-OBESITY N-ACYLETHANOLAMIDES

Catalina NEGUT,[a] Katarzyna MAKYŁA-JUZAK,[b] Oana-Iulia ENACHE[c] and Eleonora-Mihaela UNGUREANU[c*]

[a]Laboratory of Electrochemistry and PATLAB, National Institute of Research and Development for Electrochemistry and Condensed Matter, 202 Splaiul Independentei Street, 060021 Bucharest, Roumania
[b]Department of General Chemistry, Faculty of Chemistry, Jagiellonian University, Ingardena St. 3, 30-060 Cracow, Poland
[c]Politehnica University of Bucharest, 1-7 Polizu St., 011061, Bucharest, Roumania

Received February 5, 2022

The electrochemical properties of oleoylethanolamide (**O1**) have been investigated by cyclic, differential pulse and rotating disk electrode voltammetry in acetonitrile solutions. They have been compared with those of N-[2-(4-methoxyphenyl)ethyl]oleamide (**O2**) in order to find the differences between these potential anti-obesity compounds.
The physicochemical properties of **O1** and **O2** related to films formations have been thoroughly investigated at the air/water interface by means of surface pressure (π) - area (A) and electric surface potential-area isotherms. The effect of subphase temperature on the characteristics of the π-A isotherms was examined for the selected potential anti-obesity N-acylethanolamides.

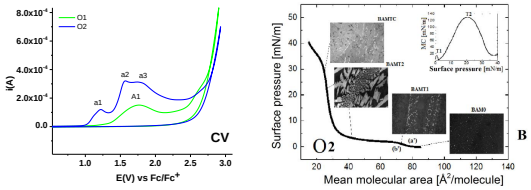

INTRODUCTION

Obesity significantly affects an increasing number of people and currently is becoming a major public health concern.[1-3] According to estimates of the World Health Organization (WHO) in 2016,[1] more than 1.9 billion adults (over 18 years old) were overweight, including 650 million people with obesity. The WHO pays special attention to the alarming fact that obesity affects a growing number of children, as evidenced of 39 million children under the age of 5 with obesity or overweight, registered in 2020. Untreated obesity can result in development of metabolic disorders (*e.g.* diabetes, hypertension), cardiovascular diseases (mainly heart disease and stroke), cancer (e.g. endometrial, breast or colon) and consequently also lead to death.[4,5] Obesity is defined as excessive fat accumulation, caused by a sedentary lifestyle, as well as eating disorders occurring as a result of other serious diseases, which can have an adverse effect on health. Treatment of obesity is being often supplemented by pharmaceutical products that limit the absorption of fat or carbohydrates, but in the long term can cause serious side effects.[6-11]

In spite of increasing knowledge about the mechanisms that control food intake and body weight, there is still no effective agents, which are safe for human health. Hence, in recent years it is observed a growing interest in the research involved in elucidating the molecular mechanism of obesity as well as developing new potent therapeutic agents that cause less side effects.

* Correspondig author: em_ungureanu2000@yahoo.com

Among different compounds with potential anti-obesity effect, oleamides are of particular interest.

The oleamides and their structural analogues belong to the group of fatty acid amides that naturally occur in food. These compounds also act as important signalling molecules with various biological effects depending on tissue type. Oleoylethanolamide (**O1**) is a fatty acid amide, which is synthesized from oleic acid and phosphatidylethanolamine mainly in brain, liver, small intestine as well as adipocyte (fat cell). [12,13] In spite of the structural similarity with oleamide, **O1** acts on peroxisome proliferator-activated receptor alpha (PPAR-α) and less on cannabinoid receptors.[14,15] The endogenous and oral/parenteral treatment with **O1** induces a satiety signal, leading to food intake decrease and body weight loss.[12, 16]

In order to search for molecules with higher activity than **O1**, other oleamides were synthesized. As example, N-[2-(4-methoxyphenyl) ethyl]oleamide (**O2**) was synthesized according to the procedure described in detail in a previous work,[17] by using a different amine.[18] Both **O1** and **O2** were compared from the point of view of physical chemical properties in order to develop new potent therapeutic agents with less side effects.

O1 and **O2** oleamides were so far biologically evaluated in the terms of the body weight variation and the food-intake by rats. The results of conducted research indicate different effects of **O1** and **O2** on the rats' treatment.[18-20] On one hand, an oral administration of **O1** to rats significantly reduced their body weight by 20.6% comparing to control group. On the other hand, an oral implementation of **O2** increased the body weight of rats and had no influence on the food intake during 10 days. In addition, an intraperitoneal administration of both **O1** and **O2** to mice showed similar favourable effects.[21]

These two N-acylethanolamides have been also used in parallel experiments designed to build stochastic sensors for carcinogenembryonic antigen (CEA) in whole blood samples, using graphite paste modified electrodes. The achieved microsensors proved to be reliable screening tools for pattern recognition of CEA and have also presented low limits of determination (0.1 pg/mL).[22] The microsensors obtained from graphite paste containing the oleamide **O2** have shown higher sensitivity (8.97×10^6 s^{-1}/mg mL^{-1}) in comparison with those containing the oleamide **O1** (1.29×10^6 s^{-1}/mg mL^{-1}). That is why, the study of these potential anti-obesity compounds is important in order to understand the differences between their behaviour and to elucidate the molecular mechanism of obesity as well.

All biochemical processes, that occur in every living cell, are closely related to its membrane structure. This makes the plasma membrane a physical medium to conduct biochemical reactions, which among other processes can be responsible for obesity.[23] One of the most promising method, that can be used to analyse properties of such biomembranes is the Langmuir monolayer technique that successfully mimic natural membrane system.[24] The application of this method in biomedical sciences is due to the fact that cellular membrane components are amphiphilic and capable to form insoluble films (Langmuir monolayers) at the air/water interface.

Therefore, the aim of presented paper is to show the results of physicochemical properties of **O1** and compare them with those of **O2** in similar electrochemical and surface absorption experiments in order to determine the source of diversity in biological activity and understand their anti-obesity effect.

RESULTS AND DISCUSSION

Electrochemical characterization of investigated oleamides

The electrochemical behaviour of compound O1 was studied on a stationary glassy carbon electrode in acetonitrile (CH_3CN) containing 0.1 M tetrabutylammonium perchlorate (TBAP) as supporting electrolyte.

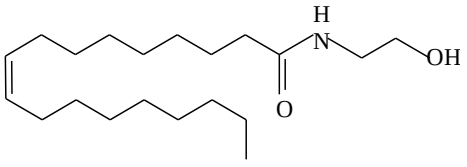

O1

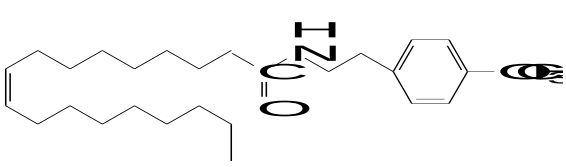

O2

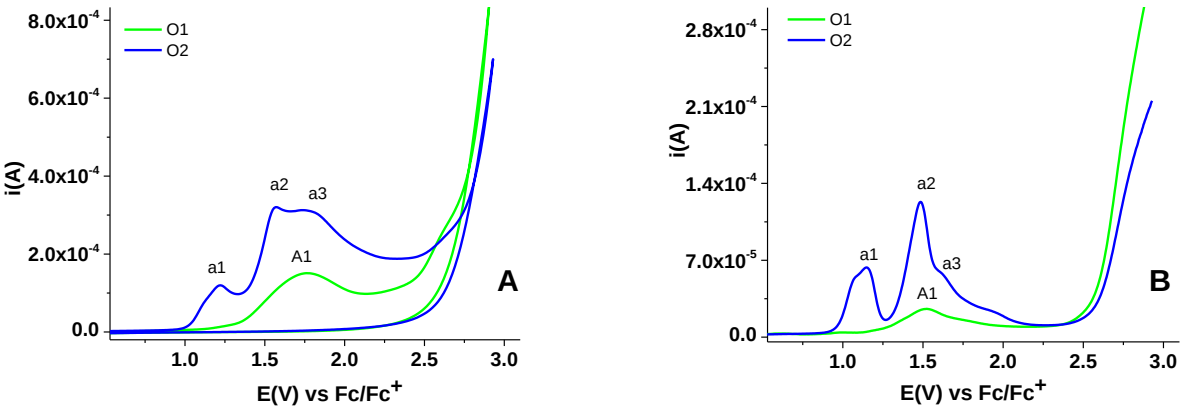

Fig. 1 – CV at 0.1 V/s (**A**) and DPV (**B**) curves for **O1** (2mM) and **O2** (2mM) in 0.1M TBAP, CH_3CN on glassy carbon electrode (3 mm diameter).

The main electrochemical experiments were carried out by cyclic voltammetry (CV) and differential pulse voltammetry (DPV). Anodic and cathodic curves were recorded individually, starting from the stationary potential. CV and DPV curves were recorded for various concentrations (0–3mM) of the studied compounds in 0.1M TBAP in CH_3CN and are presented in Fig. 1A, in comparison with that of previously studied oleamide **O2**. One large anodic (A1) peak can be noticed for **O1**, as result of more processes situated at close potential. It can be attributed to the specific oxidation process at the carbon atom from vinylic position. For **O2** three distinct processes, denoted a1, a2 and a3 have been put in evidence. No cathodic processes can be evidenced in both cases till -1.7 V.

The influences of the scan domain and scan rate on the CV curves for **O1** are presented in Fig. 2A2 and Fig. 2B2. They showed that all anodic processes are irreversible. The peak current for A1 linearly increases with the square root of the scan rate, as shown in the inset of Fig. 2B2. Figure 2B2 is an overlap of records on a cathodic potential range (0 V, -1.7 V, 0 V) and records on an anodic range (0 V, +1.7 V, 0 V). Cathodic recordings were made to show that we have no electrochemical signals in this potential range, and those in the anodic domain were made to calculate the diffusion coefficient of the compound. When calculating the diffusion coefficient, the scan rule on the same potential range was observed (0 V, +1.7 V, 0 V). The diffusion coefficients of **O1** and **O2** have been estimated from the slopes of the first oxidation peak *vs* the square root of the scan rate, using Randles-Sevcik equation (1), where: ip = peak current (A), n = number of electrons transferred in a redox cycle, F = Faraday's constant (96485.339 C/mol), R = universal gas constant (8.31447 J•K-1•mol-1), T = absolute temperature (K), A = working electrode surface area (cm2), C = molar concentration of redox-active species (mol/cm3), D = diffusion coefficient (cm2/s), v = scan rate (V/s). The values have been taken at the potential of 1.7 V, near the peak A1.

$$i_p = 0.4463\left(\frac{F^3}{RT}\right)^{1/2} n^{3/2} A D_O^{1/2} C_O^* v^{1/2} \qquad (1)$$

For one electron transfers they are: 5.2×10^{-5} and 8.7×10^{-5} cm^2/s, respectively. These values are quite surprising, as it is expected to find a higher value of diffusion coefficient (D) for **O1** (D_{O1}), because it has a smaller molecular mass than **O2**. The higher value obtained for D_{O2} can be rationalized by the fact that the molecule may adopt a special configuration that leads to increased movement speed.

A decrease of the current can be seen in successive cycles when cycling the potential in the range of O1 anodic peak A1, as shown in Fig. 3A3, showing the formation of a film or accumulation of insoluble products on the electrode surface. This behaviour is in agreement with the RDE studies (not shown) which show that for different rotation rates there is no influence of the electrode rotation rate on anodic limiting currents; this could be due to the covering of the electrode with insulating films.

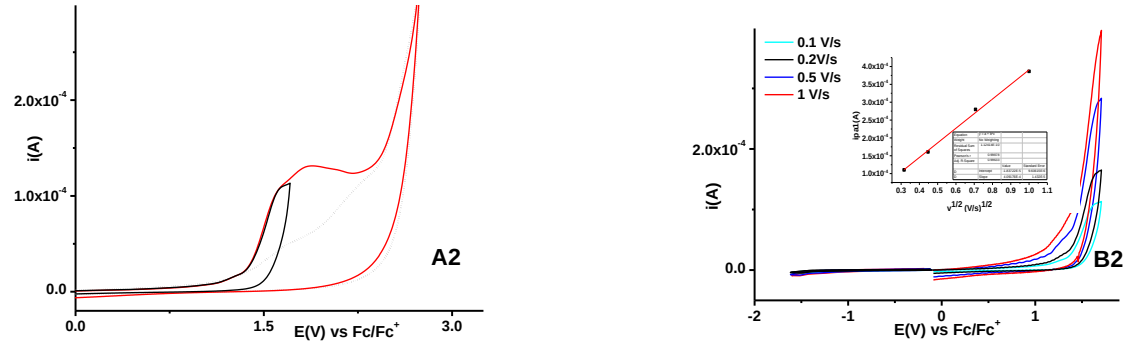

Fig. 2 – Anodic CV curves (0.1V/s) on glassy carbon electrode (3 mm diameter) on different scan domains in **O1** solutions (1 mM) in 0.1 M TBAP, CH_3CN (**A2**), and anodic and cathodic CV curves at different scan rates: 0.1; 0.2; 0.5; 1 V/s in solution of **O1** (1.5 mM) in 0.1 M TBAP, CH_3CN (**B2**); **B2** inset: dependence of the CV anodic current at 1.7 V on the square root of the scan rate.

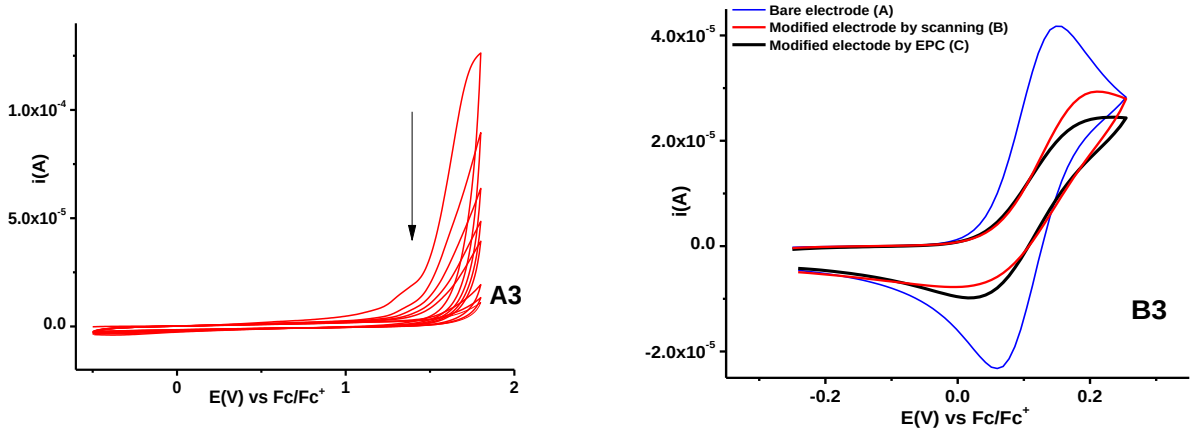

Fig. 3 – Successive CV (0.1 V/s) scans (recorded every 2 cycles during 20 cycles) on glassy carbon electrode (3 mm diameter) in **O1** solutions (3mM) in 0.1 M TBAP, CH_3CN (**A3**), and CV (0.1 V/s) curves in ferrocene solution (1mM) in 0.1 M TBAP, CH_3CN for the bare electrode (A), and for the modified electrodes obtained by scanning (B) or by CPE at 1.8 V for 2.63 mC (C) (**B3**).

After cycling the electrode potential in the range of the anodic peak A1 potential, as shown in Fig. 3A3, a chemically modified electrode (CME) is obtained. The transfer of this CME in ferrocene (Fc) solution in pure electrolyte shows altered CV curves (Fig. 3B3) for the redox probe (ferrocene), which has a typical CV on bare electrode (curve A). The electrode modification can be performed also by controlled potential electrolysis (CPE). Fig. 3B3 shows the curves obtained on different modified electrodes. The curve B was obtained for the electrode modified by 20 cycles of scanning between 0 and 1.8 V, while the curve C resulted when the CME was obtained by CPE at 1.8 V. Both B and C curves were obtained on CME obtained in rather concentrated **O1** solutions (3 mM) in 0.1 M TBAP, CH_3CN. From Fig. 3B3 it can be seen that Fc/Fc^+ couple signals are influenced by the preparation manner. The difference between the anodic and cathodic peak potentials of ferrocene is bigger on the CME (about 200 mV) than on the bare electrode (about 100 mV), confirming the electrode coverage with an insulating layer (films).

The results of investigations performed for the amide **O2** led to similar remarks on the electrochemical behaviour (anodic irreversible processes, coverage of the electrode in successive scans with formation of insulating films either by scanning or by CPE, as it was previously shown[17].

Characterization of Langmuir monolayers

Surface pressure (π)-area (A) isotherms registered for **O1** and **O2** spread on water subphase, at 20°C are presented in Fig.4. The π-A isotherm obtained for **O1** starts to rise at about 65Å^2/molecule (a). During the compression, the surface pressure increases gradually, until film collapse at above 40 mN/m (b). The course of π-A isotherm registered for **O1** indicates a liquid (L) state of the monolayer, what can be also confirmed by the

values of compression modulus (calculated according to the equation $C_s^{-1} = -A(\partial\pi/\partial A)_T$; where A denotes average area per lipid molecule in a monolayer) (Fig.4A, inset for **O1**) reaching maximum value of *ca.* 90 mN/m.[25] Additionally, the visualization of **O1** monolayer with BAM does not reveal any significant differences in the film texture during the compression.

The analysis of π-A isotherm obtained for **O2**, which starts to rise at about 80Å^2/molecule (a'), shows that upon the compression, the values of surface pressure slowly increase to reach a characteristic plateau at 2 mN/m (b'). This results in isotherm bend, that corresponds to a phase transition between liquid-expanded (LE) and liquid-condensed (LC) state of the monolayer, are widely described in literature.[26] Observed phase transition can be also confirmed by two maximum values of compression modulus: 15 mN/m corresponding to the 1st transition phase (T1 in Fig. 4B, inset) and 130 mN/m (T2 in Fig. 4B, inset) and also by changes in domain shapes observed in BAM images. Further compression of **O2** monolayer increases the surface pressure until the film collapse (collapse transition, TC) at above 25 mN/m (c') with the corresponding change of the BAM, BAMTC.

When comparing the maximum values of compression modulus as well as the values of limiting area per molecule: 45mN/m and 33mN/m for **O1** and **O2**, respectively, it can be concluded that **O1** forms a monolayer more expanded than **O2** at the air-water interface. In the case of **O2** molecule, the methoxyphenyl group bigger than hydroxyl group of **O1** is present in the structure, which is likely to cause the conformational change of the molecule, resulting in a more condensed film formed by **O2** monolayer.

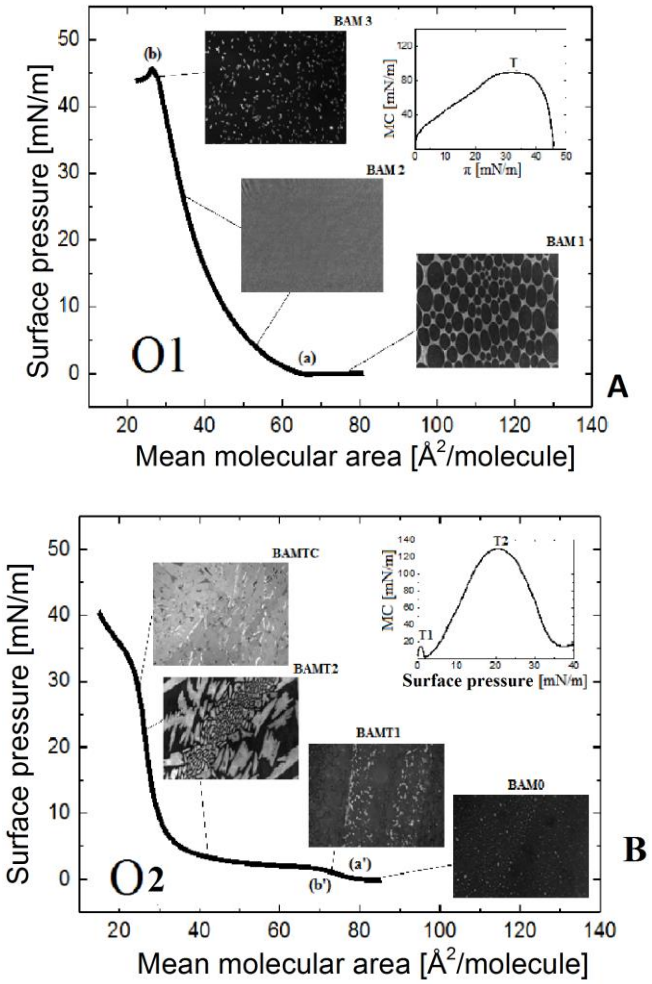

Fig. 4 – π–A isotherms of **O1** (A) and **O2** (B) spread on water subphases at 20°C with BAM images recorded during the compression. The values of compression modulus as a function of surface pressure (π) are presented in the upper right corners.

In order to provide detailed physicochemical characteristics of N-acylethanolamide monolayers, the effect of subphase temperatures on the π-A isotherms was additionally examined (Fig. 5). The shapes of π-A isotherms obtained for **O1** monolayer within the range of 10-30°C are practically parallel; however, π-A isotherm registered at 30°C is slightly shifted towards larger mean molecular areas. Conversely, the changes in subphase temperature strongly influence the course of π-A isotherms recorded for **O2** monolayer. In the case of **O2** monolayer formed on the subphase at lower temperature (10°C), the phase transition is not observed, while the increase of subphase temperature to 30°C results in a phase transition at higher surface pressure of *ca.* 15 mN/m.

For a better understanding the film forming properties of the two oleamides spread at the air/water interface, each π-A isotherm has been simultaneously recorded with the changes of electric surface potential (ΔV) (Fig. 6). Generally, the electric surface potential starts to change at slightly larger mean molecular areas (in comparison with the surface pressure), what is usually observed for film forming molecules.[27] During the compression, the electric surface potential rises gradually, reaching maximum values at the mean molecular area, that corresponds to the monolayer collapse. The maximum value of electric surface potential for **O1** monolayer was found to be 305 mV, while for **O2** monolayer was equal to 240 mV. Moreover, the course of ΔV-A isotherm recorded for **O2** monolayer is in agreement with π-A isotherm, what additionally confirms the phase transition at *ca.* 2mN/m.

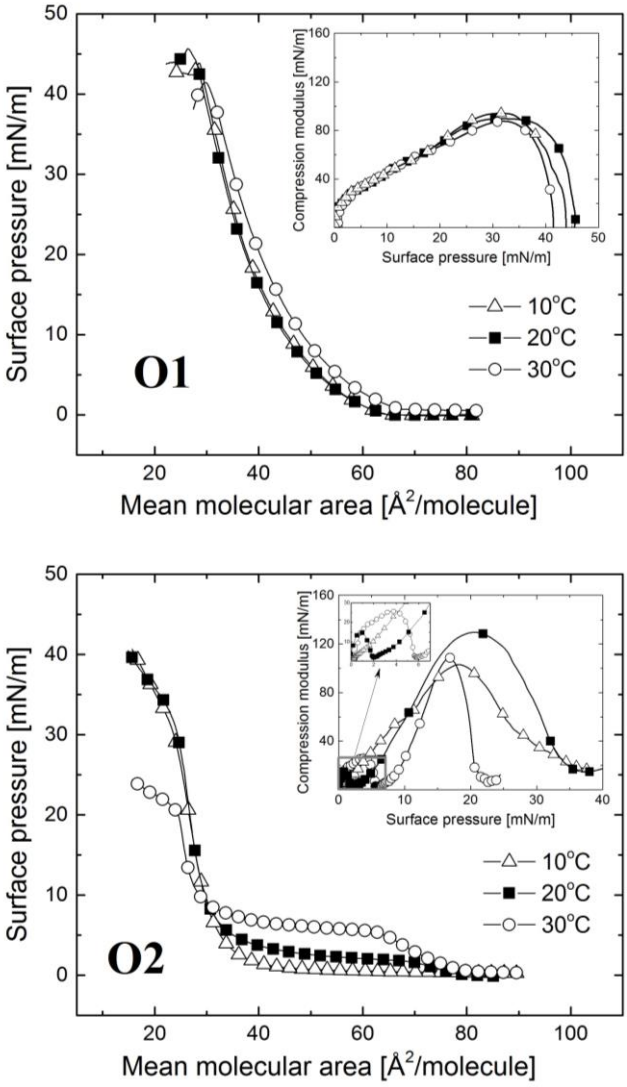

Fig. 5 – Surface pressure (π)–area (A) isotherms of **O1** and **O2** spread on water subphase at 10°C, 20°C, 30°C. The values of compression modulus as a function of surface pressure (π) are presented in the upper right corner.

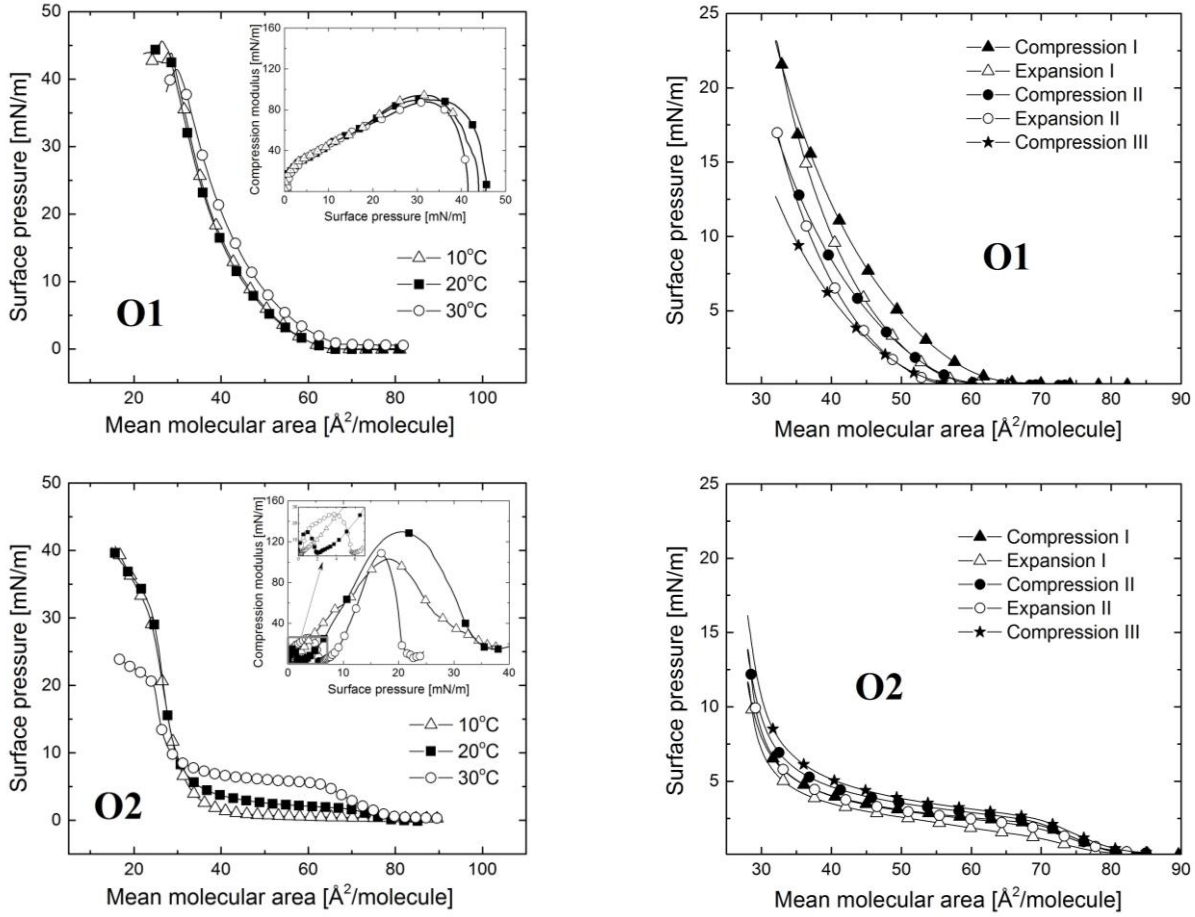

Fig. 6 – Surface pressure (π)–area (A) and electric surface potential (ΔV)–area (A) isotherms of **O1** and **O2** spread on water subphases at 20°C (left) and compression and expansion curves for **O1** and **O2** monolayers on water subphases at 20°C. The delay between consecutive cycles was 10 min.

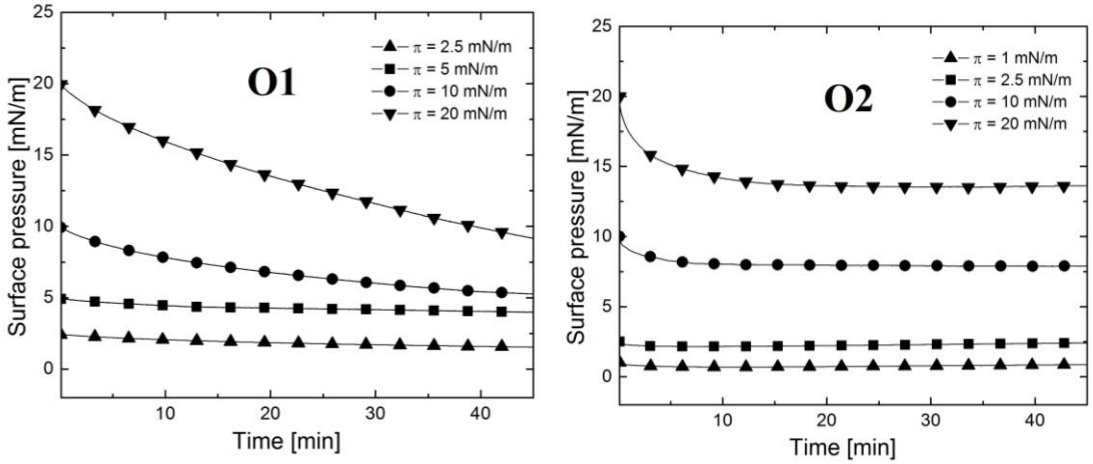

Fig. 4 – Static stability experiments of **O1** and **O2** monolayers on water subphases at 20°C.

In order to investigate the stability of oleamide monolayers each film was compressed until desired value of surface pressure (mN/m): 2.5; 5; 10; 20 and 1; 2.5; 10; 20 for **O1** and **O2**, respectively. Then monitored changes of surface pressure with time (Fig. 6) were recorded. The analysis of obtained results proved that both **O1** and **O2** form stable monolayers at the air/water interface, especially when compressed until a surface pressure up to 10 mN/m.

The stability of oleamide monolayers was also confirmed by performing hysteresis experiments

(Fig. 6), where each monolayer was compressed to a fixed surface pressure (π)-area (A) and subsequently relaxed to the original state. A target value was chosen to assure the initiation of expansion process at area values below the collapse pressure. Except for the expected loss of some film material over time, all the hysteresis curves obtained for **O1** and **O2** monolayers show similar behaviour, which also indicates their thermodynamic stability.

EXPERIMENTAL PART

Materials

Oleoylethanolamide (**O1)** and N-[2-(4-methoxyphenyl) ethyl]oleamide (**O2)** were synthesized according to the previous described method.[17] Acetonitrile (dedicated for HPLC) was used as a solvent, while tetrabutylammonium perchlorate (from Fluka) was used as a supporting electrolyte. All chemicals (except O1 and O2) were used as received. Chloroform for surface studies (dedicated for HPLC) was used as a solvent.

Apparatus and procedures

The electrochemical experiments were carried out using a PGSTAT12 AUTOLAB potentiostat coupled to a three-compartment cell. The CV curves were generally recorded at 0.1V/s or at various rates (0.1-1V/s) when studying the influence of the scan rate. DPV curves were recorded at 0.01V/s with a pulse height of 0.025V and a step time of 0.2 s. RDE experiments were performed using Autolab RDE-2 rotating disk electrode at a scan rate of 0.01V/s, with rotating rates between 500 and 1500 rpm. The working electrode was a glassy carbon disk (diameter of 3 mm). The active surface was polished before each experiment with diamond paste (2 μm), then rinsed with acetonitrile (CH_3CN). The Ag/10 mM $AgNO_3$ in 0.1 M TBAP, CH_3CN was used as reference electrode. The potential was finally referred to the potential of the ferrocene/ferricinium redox couple (Fc/Fc^+). A platinum wire was used as auxiliary electrode. The electrochemical experiments were performed at 25ºC under argon atmosphere.

For the characterization of Langmuir monolayers the spreading solutions were prepared by dissolving the investigated compounds in chloroform. The surface pressure-area (π-A) isotherms were recorded by using a KSV NIMA Langmuir through with two PTFE barriers and 841 cm^2 of its total area. Surface pressure was measured applying the methodology described elsewhere.[9] The subphase temperature was controlled thermostatically, by a circulating water system (Julabo). Spreading solutions were deposited drop by drop onto the water subphase with a Hamilton microsyringe, precise to 5.0 μL. After spreading, monolayers were left to equilibrate for 10 minutes and then compressed with barrier speed of 20 $cm^2\,min^{-1}$ while π-A isotherms were recorded.

Additionally, during the compression of selected monolayers, changes in the electric surface potential (ΔV) were measured by using KSV NIMA surface potential sensor. The vibrating plate was located *ca*. 2 mm above the water surface while the reference electrode was placed in the water subphase. Both surface pressure (π)-area (A) and electric surface potential (ΔV)-area (A) isotherms were repeated at least twice to obtain reproducible results.

In order to complement the interpretation of the obtained results, the textures of examined monolayers were studied with Brewster angle microscope (BAM) (Accurion GmbH, Germany), equipped with a 50-mW laser emitting *p*-polarized light at a wavelength of 658 nm and a 10x magnitude objective. All presented BAM images show monolayer fragments of 720 x 400 μm.

CONCLUSIONS

Irreversible anodic processes were identified by cyclic and differential pulse voltammetry for oleoylethanolamide (**O1**) and N-[2-(4-methoxyphenyl)ethyl]oleamide (**O2**). Scanning the potential in the range of the anodic peak or controlled potential electrolysis led to the coverage of electrodes with insulating layers, evidenced by ferrocene probe. The results of electrochemical studies indicate the peculiar adsorption properties of investigated oleamides. It is expected that this property allows binding of the oleamides with other compounds that may have a significant influence on excessive deposition of fat in the human body. This will be a subject of our future investigations.

The analysis of surface pressure (π)-area (A) and electric surface potential (ΔV)-area (A) isotherms registered for **O1** and **O2** shows that examined oleamides are able to form insoluble monolayers at the air-water interface. The π-A isotherms registered for **O1** monolayer are hardly influenced by the temperature conditions, whereas in the case of **O2** monolayer clearly depends on the subphase temperature. Moreover, both **O1** and **O2** molecules increase the electric surface potential of water (ΔV). These physicochemical investigations confirmed that both **O1** and **O2** are excellent film-forming material, capable to lead to stable Langmuir monolayers at the air-water interface. Furthermore, Langmuir monolayer technique allows to distinguish between physicochemical properties of these compounds at the molecular level, which was so far difficult to achieve using other methods.

Acknowledgement: This research was carried out with the equipment (BAM) purchased thanks to the financial support of the European Regional Development Fund in the framework of the Polish Innovation Economy Operational Program (Contract No. POIG.02.01.00-12-023/08). The authors are thankful to our regretted collaborator to Liviu BIRZAN, from Roumanian Academy, Organic Chemistry Center "C.D. Nenitzescu", Splaiul Independenței 202B, 71141 Bucharest, Roumania, for fruitful discussions on the topics.

REFERENCES

1. World Health Organization, Global Health Observatory, https://www.who.int/news-room/fact-sheets/detail/obesit1y-and-overweight.
2. A. D. Lopez, C. D. Mathers, M. Ezzati, D. T. Jamison and C. J. Murray, *Lancet*, **2006**, 367, 1747.
3. B. M. Popkin, "The world is fat: the fads, trends, policies, and products that are fattening the human race", Avery Trade/Penguin Group, New York, 2009.
4. P. Singla, A. Bardoloi and A. A. Parkash, *World J. Diabetes*, **2010**, *1*, 76.
5. C. S. Derdemezis, P. V. Voulgari, A. A. Drosos and D. N. Kiortsis, *Clin. Exp. Rheumatol*., **2011**, *29*, 712.
6. I. G. Smith and M. A. Goulder, *J. Fam. Pract.*, **2001**, *50*, 505.
7. A. Afshin, M. H. Forouzanfar and M. B. Reitsma, *J. Med.*, **2017**, *377*, 13.
8. S. Rossner, L. Sjostrom and R. Noack, *Obesity Research*, **2000**, *8*, 49.
9. K. M. Gadde, C. K. Martin, H. R. Berthoud, *J. Am. Coll. Cardiol.*, **2018**, *71*, 69.
10. R. S. Stafford and D. C. Radley, *Arch. Intern Med.*, **2003**, *163*, 1046.
11. M. F. Li and B. M. Cheung, *World J. Diabetes*, **2011**, *2*, 19.
12. Y. M. Al Suleimani and C. R. Hiley, *Euro. J. Pharma.*, **2013**, *702*, 1.
13. G. Petersen, C. Sorensen, P. C. Schmid, A. Hartmann, M. Tag-Christensen and S. H. Hansen, *Biochim Biophys. Acta*, **2006**, *1761*, 143.
14. J. Fu, F. Oveisi, S. Gaetani, E. Lin and D. Piomelli, *Neuropharmacology*, **2005**, *48*, 1147.
15. Y. Zhou, L. Yang, A. Ma and X. Zhang, *Neuro-pharmacology*, **2012**, *63*, 242.
16. S. Gaetani, F. Oveisi and D. Piomelli, *Neuro-psychopharmacology*, **2003**, 28, 1311.
17. C. Neguţ, E. M. Ungureanu, F. Cocu, C. Tănase, C. Draghici and C. V. Munteanu, *UPB Sci. Bull. Series*. B, **2014**, *76*, 173.
18. C. Tănase, C. Cioateş Negut, D. I. Udeanu, E. M. Ungureanu, M. Hrubaru, C. V. Munteanu, S. P. Voicu, F. Cocu and A. C. Ioniţă, *Rev. Chim.(Bucharest)*, **2014**, *65*, 768.
19. M. J. Nielsen, G. Petersen, A. Astrup and H. S. Hansen, *J. Lipid Research*, **2004**, *45*, 1027.
20. Y. Yang, M. Chen, K. E. Georgeson and M. C. Harmon, *Am. J. Physio. Regul. Integr. Comp. Physiol*., **2007**, *292*, 235.
21. C. Tanase, C. Negut, D. I. Udeanu, E. M. Ungureanu, M. Hrubaru, C. V. Munteanu, F. Cocu and R. I. Stefan van Staden, *Rev. Chim.(Bucharest)*, **2016**, *67*, 282.
22. C. Cioateş Neguţ, R. I. Ștefan-van Staden, I. Moldoveanu, E. M. Ungureanu and C. Stanciu-Gavan, *Electrochem. Commun.*, **2015**, *51*, 98.
23. G. Karp, "Cell and Molecular Biology: Concepts and Experiments", Wiley and Sons, 2004.
24. G. L. Gaines, "Insoluble monolayers at liquid-gas interfaces", Interscience Publishers, New York, 1966.
25. J. T. Davies and E. K. Rideal, "Interfacial Phenomena", Academic Press, New York, 1963.
26. J. Miñones Jr., S. Pais, J. Miñones, O. Conde and P. Dynarowicz-Łątka, *Biophys. Chem.*, **2009**, *140*, 69.
27. A. Wnętrzak, K. Łątka, M. Marzec and P. Dynarowicz-Łątka, *Acta Physica Polonica A*, **2012**, *121*, 468.
28. K. Makyła and M. Paluch, *Colloids and Surfaces B: Biointerfaces*, **2009**, *71*, 59.